Cellular Physiology and Biochemistry

Cell Physiol Biochem 2018;47:1230-1243
DOI: 10.1159/000490219
Published online: June 18, 2018
Accepted: April 17, 2018

Original Paper

Long-Term Oral Administration of Theaphenon-E Improves Cardiomyocyte Mechanics and Calcium Dynamics by Affecting Phospholamban Phosphorylation and ATP Production

Leonardo Bocchi[a] Monia Savi[a] Valeria Naponelli[b,c] Rocchina Vilella[a] Gianluca Sgarbi[d] Alessandra Baracca[d] Giancarlo Solaini[d] Saverio Bettuzzi[b,e,f] Federica Rizzi[b,e,f] Donatella Stilli[a]

[a]Department of Chemistry, Life Sciences and Environmental Sustainability, University of Parma, Parma, [b]Department of Medicine and Surgery, University of Parma, Parma, [c]Fondazione Umberto Veronesi, Milan, [d]Department of Biomedical and Neuromotor Sciences , University of Bologna, Bologna, [e]National Institute of Biostructure and Biosystems (INBB), Rome, [f]Centre for Molecular and Translational Oncology (COMT), University of Parma, Parma, Italy

Key Words
Green tea extracts • Catechins • Cardiomyocyte mechanics • Calcium dynamics • SERCA2 activity • Phospholamban • Mitochondrial respiration

Abstract
Background/Aims: Dietary polyphenols from green tea have been shown to possess cardioprotective activities in different experimental models of heart diseases and age-related ventricular dysfunction. The present study was aimed at evaluating whether long term *in vivo* administration of green tea extracts (GTE), can exert positive effects on the normal heart, with focus on the underlying mechanisms. ***Methods:*** The study population consisted of 20 male adult Wistar rats. Ten animals were given 40 mL/day tap water solution of GTE (concentration 0.3%) for 4 weeks (GTE group). The same volume of water was administered to the 10 remaining control rats (CTRL). Then, *in vivo* and *ex vivo* measurements of cardiac function were performed in the same animal, at the organ (hemodynamics) and cellular (cardiomyocyte mechanical properties and intracellular calcium dynamics) levels. On cardiomyocytes and myocardial tissue samples collected from the same *in vivo* studied animals, we evaluated: (1) the intracellular content of ATP, (2) the endogenous mitochondrial respiration, (3) the expression levels of the Sarcoplasmic Reticulum Ca^{2+}-dependent ATPase 2a (SERCA2), the Phospholamban (PLB) and the phosphorylated form of PLB, the L-type Ca^{2+} channel, the Na^{+}-Ca^{2+} exchanger, and the ryanodine receptor 2. ***Results:*** GTE cardiomyocytes exhibited a hyperdynamic contractility compared with CTRL (the rate of shortening and re-lengthening, the fraction of shortening,

L. Bocchi and M. Savi contributed equally to this work.

Donatella Stilli
and Federica Rizzi

Department of Chemistry, Life Sciences and Environmental Sustainability, University of Parmam Parco Area delle Scienze 11/A, 43124 Parma (Italy)
Tel. +39 0521906117, E-Mail donatella.stilli@unipr.it, federica.rizzi@unipr.it

the amplitude of calcium transient, and the rate of cytosolic calcium removal were significantly increased). A faster isovolumic relaxation was also observed at the organ level. Consistent with functional data, we measured a significant increase in the intracellular ATP content supported by enhanced endogenous mitochondrial respiration in GTE cardiomyocytes, as well as higher values of the ratios phosphorylated-PLB/PLB and SERCA2/PLB. ***Conclusions:*** Long-term *in vivo* administration of GTE improves cell mechanical properties and intracellular calcium dynamics in normal cardiomyocytes, by increasing energy availability and removing the inhibitory effect of PLB on SERCA2.

Introduction

Dietary polyphenols from green tea are bioactive compounds which have been shown to constitute complementary medical approaches due to their anti-cancer and cardioprotective activities. Among green tea polyphenols, known as flavanoids or catechins, the epigallocatechin-3-gallate (EGCG) is the main molecular component known to exert many biological effects [1-8].

Previous experimental studies have documented that EGCG and tea extracts are able to attenuate reperfusion-induced myocardial damage, cardiac hypertrophic response to pressure-overload, sympathetic hyperactivity in hypertension, and ventricular dysfunction in several cardiomyopathies [8-14]. Mechanistic studies have demonstrated that tea polyphenols may influence many aspects of cardiovascular function by their interaction with a list of intracellular target sites, such as several ion channels and ion exchangers (Na^+/K^+-ATPase, Na^+/H^+ and Na^+/Ca^{2+}), intracellular Ca^{2+} storage, and sarcomeric Troponin protein [7, 13, 15]. Another study reported that EGCG acute administration in cardiomyocytes, isolated from a transgenic mice model of hypertrophic cardiomyopathy, ameliorated sarcomere shortening and lowered relaxation time by decreasing the thin myofilament Ca^{2+} sensitivity [10]. More recent data also suggest an epigenetic regulation of gene expression induced by these compounds, such as inhibition of DNA methyltransferase resulting in re-activation of methylation-silenced genes, and inhibition of class I histone-deacetylases (HDAC1, HDAC2 and HDAC3) [13].

Although previous data strongly suggest that tea extracts can have benefits on cardiac function by targeting different proteins and intracellular molecular pathways, most studies refer to the effects of acute exposure to catechins and have been performed on cell lines, perfused rat hearts or isolated cardiomyocytes, subcellular cardiomyocyte organelles or in-silico models [6, 7, 15-19]. Short/long term effects of catechin treatment on heart function and ventricular remodelling have been also evaluated in experimental models of heart diseases or aged-related ventricular dysfunction [9, 13]. Conversely, studies showing potential positive effects on normal heart of long term *in vivo* administration of catechins, are still lacking.

In the present study, we specifically addressed this issue in a normal rat model, following an experimental approach which involved *in vivo* and *ex vivo* measurements of cardiac function, at different levels of complexity, from the organ to cellular levels. Hemodynamic and mechanical data were paralleled by molecular assays carried out on myocardial tissue and cardiomyocyte samples collected from the same *in vivo* studied animals, in order to evaluate (i) the effects of treatment on the cardiac Sarcoplasmic Reticulum Ca^{2+}-dependent ATPase 2a (SERCA2) and its regulatory protein Phospholamban (PLB), which regulate intracellular calcium handling and play a crucial role in cardiac contraction and relaxation, (ii) the steady-state levels of mRNA encoding the subunits of additional proteins involved in the excitation-contraction coupling, i.e. the L-type Ca^{2+} channel (CACNA1C), the Na^+-Ca^{2+} exchanger (NCX1), and the ryanodine receptor (RYR2), and (iii) the endogenous mitochondrial respiration and the intracellular content of ATP, which is the chemical currency used by cardiomyocytes to fulfil the energy demand required to sustain cell vitality and contractile function.

Materials and Methods

Animals and experimental protocol

This study was carried out in strict accordance with the recommendations in the Guide for the Care and Use of Laboratory Animals (National Institute of Health, Bethesda, MD, USA, revised 1996). The investigation was approved by the Veterinary Animal Care and Use Committee of the University of Parma-Italy (Prot. N° 614/2016-PR) and conforms to the National Ethical Guidelines of the Italian Ministry of Health. All efforts were made to minimize animal suffering.

The study population consisted of 20 male Wistar rats (Rattus norvegicus) aged 12-14 weeks, weighing 414 ± 9.6 g (mean ± standard error of the mean), individually housed in a temperature-controlled room at 22-24°C, with the light on between 7.00 AM and 7.00 PM. The bedding of the cages consisted of wood shavings and food was freely available. We previously verified that 40 mL corresponded to the lowest value of the range of daily water consumption in male rats, matched for age and body weight. Accordingly, ten animals were given 40 mL/day tap water solution of green tea extracts (Theaphenon-E, concentration 0.3%; Theaphenon-E was kindly provided by Tea Solutions, Hara Office Inc., Japan) for 28 days (GTE group). The remaining ten animals received the same volume of water and were used as controls (CTRL group). As expected, all the GTE animals consumed the entire volume of solution and thus the same amount of substance.

The components green tea extracts included: epigallocatechin gallate (68.58%), epigallocatechin (10.56%), epicatechin gallate (5.95%), epicatechin (4.31%), gallocatechin gallate (1.23%), DL-catechin (0.56%), caffeine (0.44%), and traces of theobromine and gallic acid. Body weight was measured once a week until sacrifice, after 4 weeks of treatment. As shown in Table 1, body weight exhibited only minor changes during the experimental protocol. Specifically, in CTRL, a slight increase (less than 10%) was observed at the fourth week. In GTE animals, the body weight remained practically constant, despite a transitory negligible decrease (approximately 5%) during the first week of treatment. No significant differences were observed between the two experimental groups, at the time points considered (Table 1).

Before sacrifice, hemodynamic data were invasively recorded from anaesthetized CTRL and GTE rats. Then, in selected subgroups of animals (6 CTRL and 6 GTE), the heart was excised and cardiac cells were enzymatically isolated to measure cardiomyocyte mechanical properties and calcium transients (sub heading *Cell cardiomyocyte mechanics and Ca^{2+} transients).*

A fraction of isolated cardiomyocytes was washed three times with low-calcium solution (0.1 mM) and centrifuged (500 rpm for 5 min). After removing the supernatant, the pellet was stored at -80 °C for the subsequent evaluation of ATP content (subheading *ATP content analysis in LV cardiomyocytes)*. From the remaining four rats, the heart was rapidly excised and perfused with a 0.9% NaCl solution at 37 °C to drain the residual blood. Then, the tissues (left and right ventricles) were wiped with filter paper, mechanically fragmented in liquid nitrogen and stored at -80 °C for molecular analyses (subheadings *Protein extraction, quantification, electrophoresis and Western blot analysis,* and *RNA extraction, retrotranscription and RT-qPCR analysis*).

To clarify whether GTE exerts some effects on cardiomyocyte mitochondrial function, possibly attributable to EGCG, sixteen additional rats were studied, including GTE-treated rats (n=4), EGCG-treated rats (n=4), and control animals (n=8), by applying the same dosing schedule previously described. EGCG was given in amounts equivalent to the EGCG content in total GTE *(*subheading *Cell respiration measurements).*

Hemodynamic study

Each animal was anaesthetized with ketamine chloride (Imalgene, Merial, Milan, Italy; 40 mg/kg i.p.) plus medetomidine hydrochloride (Domitor, Pfizer Italia S.r.l., Latina, Italy; 0.15 mg/kg i.p.). Invasive hemodynamic data were recorded with the aid of a microtip pressure transducer catheter (Millar SPC-320, Millar Instruments, Houston, TX, USA) connected to a recording system (Power Laboratory ML 845/4 channels, 2Biological Instruments, Besozzo, Italy). After

Table 1. Body weights (g). Mean values ± SEM of body weights measured once a week, in un-treated (CTRL) and treated (GTE) animals

	CTRL	GTE
Day 0	414.7 ± 12.2	417.8 ± 11.4
Day 7	423.4 ± 8.8	402.3 ± 14.5
Day 14	432.6 ± 7.8	412.0 ± 13.9
Day 21	437.8 ± 7.2	415.4 ± 15.2
Day 28	441.1 ± 7.4	422.3 ± 15.7

measuring systolic and diastolic blood pressure into the right carotid artery, the catheter was advanced into the left ventricle to measure the following parameters: (1) left ventricular (LV) systolic pressure (LVSP), (2) LV end-diastolic pressure (LVEDP), (3) the peak rate of rise and decline of LV pressure ($\pm dP/dt_{max}$), taken as indexes of ventricular mechanical efficiency, (4) isovolumic contraction time (IVCT: duration of isovolumic contraction), (5) total cycle duration (Tcycle), and (6) heart rate (HR) (software package AcqKnowledge 3.9; Biopac Systems, Goleta, CA).

Cardiomyocyte mechanics and Ca^{2+} transients

From the heart of 6 CTRL and 6 GTE, individual LV myocytes were enzymatically isolated by collagenase perfusion, in accordance with a procedure previously described [20].

Mechanical properties of freshly isolated ventricular myocytes were assessed by using the IonOptix fluorescence and contractility systems (IonOptix, Milton, MA, USA). LV myocytes were placed in a chamber mounted on the stage of an inverted microscope (Nikon-Eclipse TE2000-U, Nikon Instruments, Florence, Italy) and superfused (1 mL/min at 37°C) with a Tyrode solution containing (in mM): 140 NaCl, 5.4 KCl, 1 $MgCl_2$, 5 HEPES, 5.5 glucose, and 1 $CaCl_2$ (pH 7.4, adjusted with NaOH) (all chemicals from Sigma-Aldrich, Milan, Italy). Only rod-shaped myocytes with clear edges and average sarcomere length ≥ 1.7 μm were selected for the analysis, using a 40X oil objective lens (NA: 1.3). All the selected myocytes did not show spontaneous contractions. The cells were field stimulated at a frequency of 0.5 Hz by constant current pulses (2 ms in duration, and twice diastolic threshold in intensity; MyoPacer Field Stimulator, IonOptix). Load-free contraction of myocytes was measured with the IonOptix system, which captures sarcomere length dynamics via a Fast Fourier Transform algorithm. A total of 216 isolated ventricular myocytes were analysed (82 from CTRL hearts and 134 from GTE) to compute the following parameters: mean diastolic sarcomere length, fraction of shortening (FS), time to peak shortening (TPS), maximal rates of shortening ($-dl/dt_{max}$) and re-lengthening ($+dl/dt_{max}$), and time to 10% and 50% of re-lengthening (RL10%, RL50%). Steady-state contraction of myocytes was achieved before data recording by means of a 10 s conditioning stimulation. Sampling rate was set at 1 kHz.

In a subgroup of 40 CTRL and 40 GTE cells, Ca^{2+} transients were measured simultaneously with mechanical properties. Ca^{2+} transients were determined by epifluorescence after loading the myocytes with 10 μM fluo 3-AM (Invitrogen, Carlsbad, CA) for 30 min. Excitation wavelength was 480 nm, with emission collected at 535 nm. Fluo 3 signals were expressed as normalized fluorescence (f/f0: fold increase). The time course of the fluorescence signal decay was described by a single exponential equation, and the time constant (tau) was used as a measure of the rate of intracellular calcium clearing [21]. The time to peak of the calcium transient (TTP) was also measured in order to indirectly assess potential effects of GTE treatment on ryanodine receptors.

Detection of intracellular Ca^{2+} level

To detect the intracellular Ca^{2+} concentration, one mL suspension of isolated cardiomyocytes was incubated with 2.0 μM fura-2-acetoxymethyl ester (Invitrogen by Thermo Fisher Scientific, Waltham, MA, USA) plus Pluronic (0.04%; Sigma) for 10 min, at room temperature. Then, cardiomyocytes were washed twice with low calcium (0.1 mM) solution to remove the remaining fura-2 and complete the de-esterification of intracellular Acetoxymethyl (AM) ester.

The loaded cells were placed in a perfusion chamber on the stage of an inverted microscope (Olympus IX71) and superfused (1 mL/min at 37°C) with a Tyrode solution containing (in mM): 140 NaCl, 5.4 KCl, 1 MgCl2, 5 HEPES, 5.5 glucose, and 1 CaCl2 (pH 7.4, adjusted with NaOH) (all chemicals from Sigma-Aldrich, Milan, Italy). The intracellular Ca^{2+} transients were measured with contractility recording system (IonOptix LLC, Milton USA) at 0.5 Hz pacing rate (field stimulation). Cells were excited at 360/380 nm and emission was measured at 510 nm. The ratio of the fluorescence emitted by 360 nm and 380 nm excitation was used as an indicator of intracellular free Ca^{2+} (ΔF360/380). The Ionwizard software (IonOptix) was used to capture the changes of fura-2 fluorescence intensity. Then, the actual intracellular calcium ion concentration was computed by applying *in vitro* calibration, according with the manufacturer's instructions (IonOptix).

Cell respiration measurements

Respiratory rates of LV cardiomyocytes isolated from the hearts of control, GTE and EGCG-treated rats, were assayed at 30°C using a Clark-type oxygen electrode, essentially according with a method previously described [22]. Mitochondrial respiration was determined in intact cells suspended in the isolation buffer,

containing 22 mM glucose and 5 mM pyruvate as energy substrates. The endogenous respiration was sensitive to rotenone and antimycin A. Cells were counted by using the MUSE cell analyzer (Millipore, Billerica, MA, USA) and the activities were expressed as nmol/min/10^6 cells.

ATP content analysis in LV cardiomyocytes

The ATP intracellular content was measured by the Luminescence ATP Detection Assay System (ATPlite) (PerkinElmer, Waltham, MA, USA) according to the manufacturer's protocol. Briefly, a frozen pellet of isolated LV cardiomyocytes was re-suspended in 1 mL of PBS and 10 µL of this suspension was further diluted to a final volume of 600 µL with PBS. Aliquots of 100 µL of diluted cell suspension were pipetted in quadruplicate in a 96-well white plate. Then, 50 µL/well of mammalian cell lysis solution were added and the plate was shaken at 700 rpm for 5 minutes in an orbital shaker before to add 50 µL/well of substrate solution. The microplate was shaken again for 5 minutes and dark incubated for 10 minutes. The luminescence intensity was then measured by the EnSpire® multimode plate reader (PerkinElmer). The row luminescence data were normalized for the total protein content of each sample, determined by the DC Protein assay kit (Bio-Rad, Hercules, CA, USA).

Protein extraction, quantification, electrophoresis and Western blot analysis

GTE-treated and control rat ventricles were ground in liquid nitrogen to a fine powder; 30 mg were used to extract proteins in 500 µL of ice-cold modified RIPA buffer (50 mM Tris- HCl pH 7.4, 100 mM NaCl, 1% Triton X-100) supplemented with adequate amount of protease and phosphatase inhibitor cocktails (Sigma-Aldrich). Extracts were centrifuged (14000 rpm for 30 min at 4 °C) and supernatants were stored at -20 °C. Protein concentration was estimated by the DC Protein assay kit (Bio-Rad) using bovine serum albumin (Sigma-Aldrich) as a standard. The equivalent of 75 µg of total lysate was incubated for 30-40 minutes at 37 °C before being loaded and resolved by 15% acrylamide SDS-PAGE. For western blot analysis, proteins were electrophoretically transferred, overnight at 4 °C, to PVDF membranes (EMD Millipore, Merk KGaA, Darmstadt, DE). Transfer efficiency was routinely monitored by 0.1% Ponceau S staining (Sigma-Aldrich). Blotted membranes were incubated with TBS-T buffer (50 mM Tris-HCl pH 7.5, 150 mM NaCl, 0.1% Tween 20) containing 5% (w/v) non-fat dry milk powder for 3 or 6 hours at room temperature with gentle shaking. Membranes were probed overnight at 4 °C with the primary antibodies diluted in TBS-T containing 5% (w/v) non-fat dry milk. The following antibodies were used: rabbit polyclonal anti-phospho-Phospholamban (Ser16), dilution 1:200, from Millipore (EMD Millipore Corporation, Temecula, CA); mouse monoclonal anti-Phospholamban (2D12), dilution 1:1000, and rabbit polyclonal anti-SERCA2 ATPase, dilution 1:1000, from Abcam (Cambridge, UK) and mouse monoclonal anti-β actin, dilution 1:500, from Santa-Cruz Biotechnology (Santa Cruz, CA, USA). After extensive washes with TBS-T, membranes were incubated with horseradish peroxidase-conjugated anti-mouse (dilution 1:5000) or anti-rabbit (dilution 1:200000) secondary antibodies (Sigma-Aldrich) diluted in TBS-T containing 5% (w/v) non-fat dry milk for 1 hour at room temperature. Immunoreactive bands were detected using the BM Chemiluminescence Western Blotting Substrate (Hoffmann-La Roche, Basel, Switzerland) and quantified by the Quantity Basic analysis software (BioRad).

RNA extraction, retrotranscription and RT-qPCR analysis

GTE and CTRL rat ventricles were ground in liquid nitrogen to a fine powder; about 30 mg of powder were dissolved in 1 mL of TRIZOL reagent (Thermo Fisher Scientific, Waltham, MA, USA) and used for RNA purification with the PureLink RNA Mini kit (Thermo Fisher Scientific). For reverse transcription reaction, RevertAid First Strand cDNA Synthesis kit (Thermo Fisher Scientific) was used following the manufacturer's instructions. Briefly, 1 µg of total RNA for each sample was combined with 1 µL of Oligo dT Primers (100 µM) and heated at 65 °C for 5 min. After a quick chill on ice the first strand synthesis reaction was carried out for 60 min at 42 °C and stopped at 70 °C for 5 min. Two µL of each cDNA preparation diluted 1:2 in water were used for RT-qPCR with the set of primers described in Table 2, using SSOAdvanced Universal SYBR Green Supermix (Bio-Rad) and performed in duplicate on the DNA Engine Opticon 4 (MJ Research, Walthman, MA, USA). Thermal cycler conditions consist of an initial denaturation at 95 °C for 30 sec followed by 40 cycles of denaturation at 95 °C for 15 s and annealing and extension at 60 °C for 20 s.

Primer pair for SERCA2 was designed using the NM_001110139.2 GenBank sequence by means of PrimerBLAST (NCBI; www.ncbi.org/bast/primerblast). RYR2 primers were freely accessible in RTPrimerDB database (http://www.rtprimerdb.org).

The cycle threshold (Ct), that is defined as the number of cycles required for the fluorescent signal to cross the threshold, was determined for each gene in all the samples and normalized for the Ct value of the reference gene glyceraldehyde phosphate dehydrogenase (GAPDH) measured in the same sample: normalized Ct =Ct (target gene) – Ct (GAPDH).

Table 2. Primer sequences

Gene	Forward primer sequence	Reverse primer sequence
GAPDH [23]	5′ GTTCCAGAGACAGCCGCATC 3′	5′ CGTTCACACCGACCTTCACC 3′
PLN [23]	5′ CATGCCAACGCAGTTACAACCT 3′	5′ TCGTGACCCTTCACGACGAT 3′
NCX1 [23]	5′ CGAAATGGATGGGAAAGTAGTCAAC 3′	5′ TCTTTGTCGGGATGCTTCTGC 3′
SERCA2	5′ AACTACCTGGAGCCTGCAAT 3′	5′ TTCCCCAAGCTCAGTCATGC 3′
CACNA1C [24]	5′ ATGGTTCTTGTCAGCATGTTGCGG 3′	5′ TGCAAATGTGGAACCGGTGAAGTG 3′
RYR2	5′ GGCGGAATTTCTTGCCAAC 3′	5′ CCTCGCACCTCATCCTGAGT 3′

Statistical analysis

The IBM SPSS statistical package (International Business Machines Corporation, Armonk, NY,

USA, version 24) was used. Normal distribution of variables was checked by means of the Kolmogorov-Smirnov test. Statistics of variables included mean ± standard error of the mean (SEM), unpaired Student's t test (hemodynamics), General Linear Model (GLM) ANOVA for repeated measurements (cell mechanics, Ca^{2+} transients, and ATP content analysis), non-parametric statistical test U-Mann Whitney (western blot data and RT-qPCR data), and one-way ANOVA followed by the Bonferroni's post-hoc test (mitochondrial respiration rates analysis). Details on the specific test used are reported in the Fig. legend of each specific experiment. Statistical significance was set at $p<0.05$.

Table 3. Hemodynamic study. Mean values ± SEM of blood pressure (BP), left ventricular (LV) systolic pressure (LVSP), left ventricular end-diastolic pressure (LVEDP), maximal rate of LV pressure rise ($+dP/dt_{max}$), maximal rate of LV pressure decline ($-dP/dt_{max}$), isovolumic contraction time (IVCT), and total cycle duration (Tcycle). * $p<0.05$ vs CTRL (unpaired Student's t test)

	CTRL (n=10)	GTE (n=10)
Systolic arterial BP (mmHg)	131.9 ± 4.89	134.4 ± 4.39
Diastolic arterial BP (mmHg)	103.5 ± 2.15	104.7 ± 2.96
LVSP (mmHg)	138.5 ± 5.75	138.6 ± 5.58
LVEDP (mmHg)	5.60 ± 0.41	4.62 ± 0.37
$+dP/dt_{max}$ (mmHg/s)	7358.2 ± 222.7	7368.6 ± 183.6
$-dP/dt_{max}$ (mmHg/s)	-6605.1 ± 269.1	-7592.4 ± 263.2 *
IVCT (s)	0.021 ± 0.0004	0.021 ± 0.0006
Tycle (s)	0.140 ± 0.006	0.138 ± 0.005

Results

Hemodynamics

Heart rate measured in anaesthetized rats did not show substantial differences between GTE and CTRL animals (range 185-251 beats/min in CTRL, 195-276 beats/min in GTE rats). Although the average values of most parameters relating to hemodynamic performance were comparable in the two experimental groups, a significant increase in the maximal rate of left ventricular pressure decline ($-dP/dt_{max}$) during isovolumic relaxation was observed in GTE-treated group (+15%, $p<0.05$; Table 3).

Cardiomyocyte mechanics and calcium transients

More evident effects of GTE treatment were observed when the intrinsic mechanical properties and intracellular calcium dynamics were analyzed, in unloaded isolated cardiomyocytes (Fig. 1A-J). In the absence of marked changes in the average diastolic sarcomere length (1.781 ± 0.004 μm in CTRL; 1.782 ± 0.003 μm in GTE cells), GTE cardiomyocytes exhibited a significant increase in the fraction of shortening (FS, Fig. 1C), and in the maximal rate of shortening ($-dl/dt_{max,}$ Fig. 1D) and re-lengthening ($+dl/dt_{max,}$ Fig. 1F), resulting in a lower time to peak shortening (TPS, Fig. 1E) and shorter relaxation times as measured at 10% and 50% of re-lengthening (RL10% and RL50%, Fig. 1G). Consistent with data related to cell mechanics, an improved efficiency of the mechanisms involved in the intracellular calcium

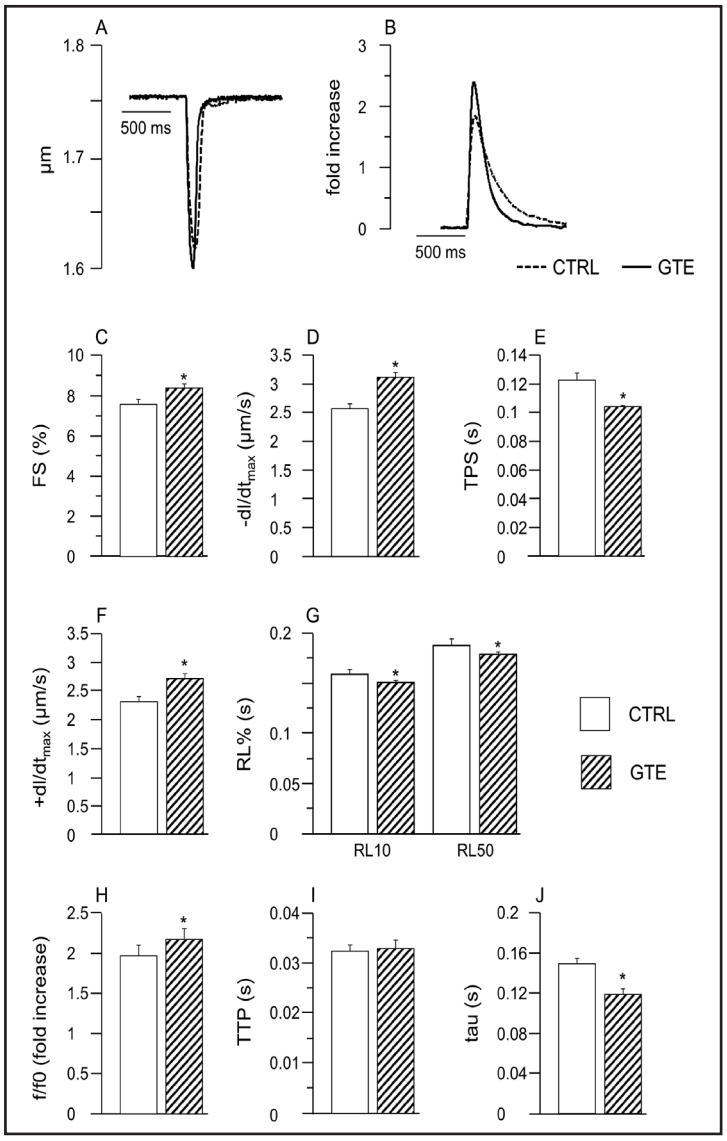

Fig. 1. Effects of GTE on cell mechanics and intracellular calcium dynamics. Representative examples of sarcomere shortening (A) and calcium transients (B, normalized traces: fold increase) recorded from CTRL (dashed line) and GTE (solid line) ventricular myocytes. In bar graphs C-J: Mean values ± SEM of sarcomere shortening (C, FS), maximal rate of shortening (D, $-dl/dt_{max}$), time to peak shortening (E, TPS), maximal rate of re-lengthening (F, $+dl/dt_{max}$), time to 10% and 50% re-lengthening (G, RL10% and RL50%), calcium transient amplitude expressed as peak fluorescence normalized to baseline fluorescence (H, f/f0), time to peak of the calcium transient (I, TTP), and time constant of the intracellular calcium decay (J, tau), measured in CTRL (82 and 40 cells, for mechanics and calcium transients respectively) and GTE cells (134 and 40 cells). * $p<0.05$ significant differences vs CTRL (GLM-ANOVA for repeated measurements).

handling was observed in GTE group, as documented by the higher amplitude of the calcium transient (f/f0, Fig. 1H), associated with lower values of *tau* (tau, Fig. 1J), indicating a faster cytosolic calcium removal. Conversely, the time to peak of the calcium transient exhibited comparable values in CTRL and GTE cardiomyocytes (TTP, Fig. 1I). Noteworthy, the diastolic calcium levels exhibited comparable values in the two groups of cells, as measured after loading an aliquot of the cardiomyocyte suspension with 2.0 µM fura-2-acetoxymethyl ester (Fig. 2).

ATP content analysis in LV cardiomyocytes

A significant increase in the intracellular ATP content was measured in GTE cardiomyocytes as compared with CTRL (+25%, $p<0.001$; Fig. 3). This finding can at least partially explain the higher contractile efficiency observed in GTE cells, by considering that (i) local energetic control is essential for the functioning of the two major cardiomyocyte ATPases involved in the contraction-relaxation processes, i.e. SERCA2 and the myosin ATPase, and (ii) changes in ATP content are associated with parallel variations in cardiomyocyte ATPase activity [25, 26].

Mitochondrial respiration assay in LV cardiomyocytes

To verify whether the observed increase in intracellular ATP was due to an EGCG mediated effect on mitochondria, we measured the endogenous oxygen consumption rate of

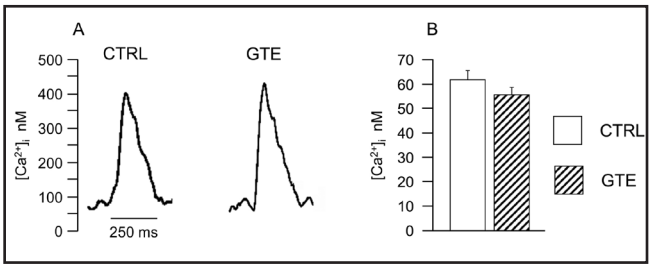

Fig. 2. Intracellular diastolic Calcium levels. (A) Representative analog recordings of calcium transients measured in CTRL and GTE cells, after incubation with 2.0 μM fura-2-acetoxymethyl ester. (B) Mean values ± SEM of diastolic intracellular calcium concentration in the two groups of cardiomyocytes.

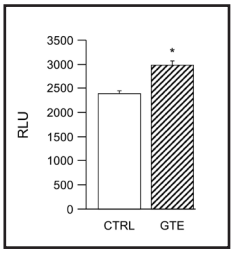

Fig. 3. Effects of GTE on cardiomyocyte ATP content. Mean values ± SEM of ATP content in control (CTRL) and GTE left ventricular myocytes. Values are expressed as relative light units (RLU), counts/s. * p<0.001 vs CTRL (GLM-ANOVA for repeated measurements).

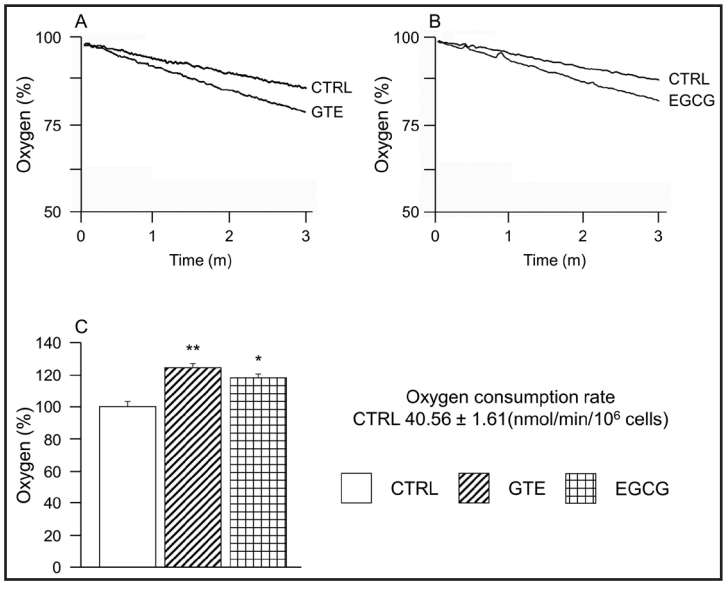

Fig. 4. Respiration measurements in intact rat cardiomyocytes. A-B: Typical oxygen consumption traces in GTE (A), and EGCG (B) cells compared to CTRL. Oxygen concentration at 30 °C is 204.1 μM (100 % saturation). C: bar graph showing the mean values ± SEM of the oxygen consumption rate percentage changes of treated cells as compared with CTRL cardiomyocytes. * p<0.05, ** p<0.01 statistically significant differences vs CTRL (one-way ANOVA and Bonferroni post-hoc test).

cardiomyocytes isolated from EGCG-treated and GTE-treated rats (Fig. 4A-C). A significant enhancement of the respiration rate was observed in both GTE and EGCG cardiomyocytes compared to CTRL (+ 24% p<0.01 and +18% p<0.05, respectively; Fig. 4C), indicating that both treatments induced a significant increase of the oxidative phosphorylation activity in cardiomyocytes.

Electrophoresis and Western blot analysis: SERCA2, PLB, and p-PLB expression.

The expression levels of SERCA2 were comparable in CTRL and GTE (Fig. 5A). SERCA2 activity is mainly modulated by a small protein, the PLB. The phosphorylation status of PLB (p-PLB) is able to remove the inhibitory effect of PLB on SERCA2, resulting in increased SR-Ca^{2+} uptake and enhanced myocyte contractility and relaxation [27]. We have actually measured a marked decrease in the total PLB (-23%, p=0.08; Fig. 5B) associated with a more evident increase in the phosphorylated form of the protein (+58%, p-PLB, p=0.08; Fig. 5C), resulting in a significant increase in the p-PLB/PLB ratio (+100%, p<0.05; Fig. 5D). Consistent with this finding, a more efficient intracellular calcium dynamics and improved cardiomyocyte contractility were observed in GTE cells. Noteworthy, GTE cells also exhibited a significantly higher SERCA2/PLB ratio compared with CTRL (+15%; p<0.05; Fig. 5E) which

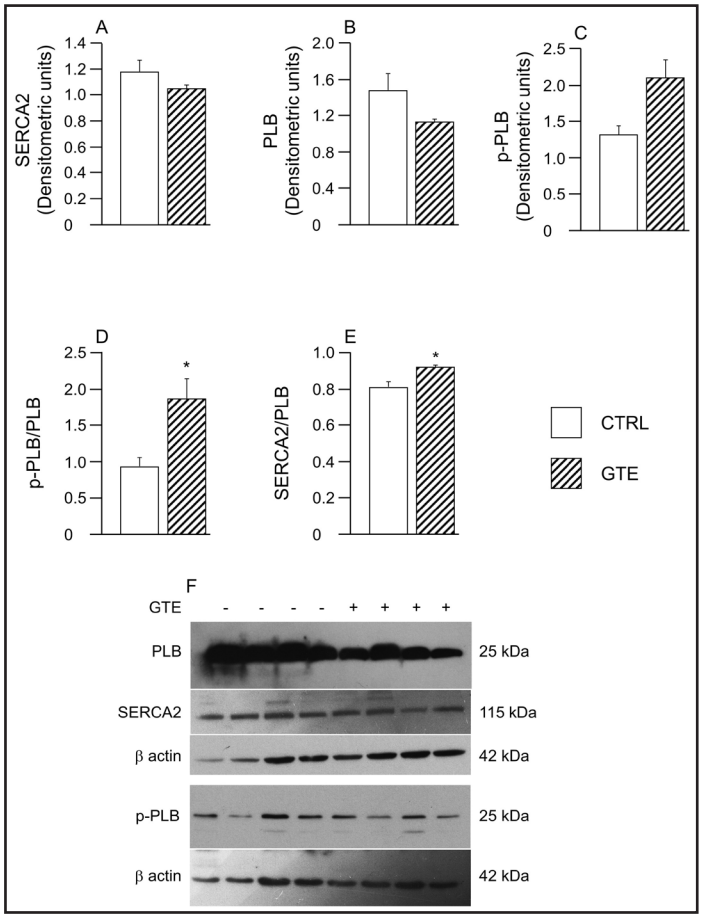

Fig. 5. GTE-induced effects on SERCA2 and PLB protein expression. Average values ± SEM of SERCA2 (A), PLB (B), p-PLB (C) expression levels normalized to β-actin, measured by immunoblot assay in the ventricular myocardium of CTRL (n=4) and GTE (n=4) groups. Data are expressed in densitometric units. In bar graphs D-E: p-PLB/PLB ratio (D) and SERCA2/PLB ratio (E). * $p<0.05$ significant differences vs CTRL (U-Mann Whitney statistical test). In F: sets of immunoreactive bands related to PLB, SERCA2 and p-PLB expression, in GTE and CTRL ventricular tissue. Aspecific bands of SERCA2 and p-PLB were excluded from the densitometric calculation. The western blots are representative of three different experiments showing similar results.

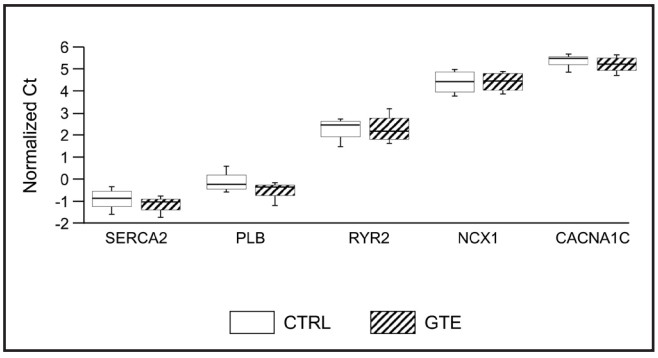

Fig. 6. Box plot of gene expression data measured by RT-qPCR. Box plot distribution of the Ct values of SERCA2, PLB, RYR2, NCX1 and CACNA1C, normalized to the Ct of GAPDH. A higher normalized Ct value means lower gene expression levels. Negative Ct values mean that the target gene is more expressed than GAPDH. Ventricular tissue samples analysed for gene expression: CTRL (n=4) and GTE (n=4). Statistical analysis was performed by U-Mann Whitney test.

has been linked to an increased SERCA2 affinity for Ca^{2+} [28, 29] and may further contribute to enhance the mechanical efficiency of GTE-treated cardiomyocytes.

RT-qPCR analysis: SERCA2, PLB, NCX1, RYR2 and CACNA1C mRNA expression

In order to verify whether GTE transcriptionally modulates the expression of proteins involved in the excitation-contraction coupling, we performed a RT-qPCR assay for measuring the steady-state levels of mRNA encoding the subunits of SERCA2, PLB, L-type Ca^{2+} channel (CACNA1C), Na^{+}-Ca^{2+} exchanger (NCX1), and ryanodine receptor (RYR2). As already observed at the protein level, the expression of SERCA2 and PLB mRNA were comparable in CTRL and GTE (Fig. 6). Furthermore, we did not find statistically significant changes in the expression of CACNA1C, NCX1, and RYR2 in the ventricular samples obtained from GTE-treated rats in comparison with controls.

Discussion

In the present study we provide evidence that long-term *in vivo* oral administration of GTE can improve cell mechanical properties and intracellular calcium dynamics in normal cardiomyocytes, by affecting the two major players involved in the contraction-relaxation processes, i.e. cardiomyocyte energy production and the phosphorylation state of PLB, the small protein modulating the SERCA2 activity, without changes in the calcium sensitivity of ryanodine receptors and the expression levels of proteins involved in the intracellular calcium handling, as measured at mRNA level (SERCA2, PLB, L-type Ca^{2+} channel, Na^{+}-Ca^{2+} exchanger, and ryanodine receptor) and protein level (SERCA2, PLB).

A standardized GTE was used in our study instead of pure EGCG or single catechins. EGCG is undoubtedly the most abundant catechin in GTE and the most studied one, however it is still a matter of debate whether other catechins or their metabolites may contribute to ameliorate EGCG bioavailability or have additive biological effects [30, 31]. Also, GTE is chemically more stable than pure EGCG, due to the presence of other antioxidant protective constituents [32]. We did not measure plasma concentration of catechins in our experimental model. However, a detailed quantification of plasma and tissue levels of catechins in rats drinking a GTE preparation of analogue composition, administered following our same dosage schedule, was already provided by Kim et colleagues [33]. These authors found that total epigallocatechin (EGC) and epicatechin (EC) plasma concentration ranged from 300 to 1000 ng/mL during the 4 weeks period. Total EGCG plasma levels were significantly lower (50-200 ng/mL), but still clearly detectable. All the catechins were detected in many body tissues, including the heart, at a concentration of ng/g of tissue (EGC: 30±7 ng/g; EC: 21±6; EGCG: 3.5±0.4) [33].

We observed a significant increase in the intracellular ATP content associated with higher levels of phosphorylated PLB (p-PLB) in functional cardiomyocytes isolated from rats receiving GTE in drinking water in comparison to water fed controls. Consistent with these data, GTE cardiomyocytes exhibited a hyperdynamic contractility, an increased calcium transient amplitude and a more efficient cytosolic calcium removal, associated with a faster isovolumic relaxation, as measured at the organ level.

The intracellular total ATP content represents the balance value between ATP production and ATP consumption in a certain moment, and the primary energy source in the heart tissue is the mitochondrial oxidative phosphorylation. The increased ATP content in GTE cardiomyocytes is in accordance with previous studies showing that EGCG, the most abundant component of GTE, enhances ATP production by acting on mitochondria, as well as on 5′-AMP kinase (AMPK), probably the most important cytosolic energy sensing enzyme, that promotes ATP production by switching on the catabolic processes while switching off the anabolic pathways [34]. In human cultured neurons, EGCG was capable to increase ATP production by promoting mitochondrial respiration and oxidative phosphorylation through cytochrome C oxidase (CcO) activation [35]. A positive effect of EGCG on the mitochondrial capacity to produce energy has been also documented *in vivo*. In elder rats receiving by oral gavage 2 mg/kg/day EGCG for 30 days, the activities of both the mitochondrial enzymes of the tricarboxylic acid cycle (TCA) and the mitochondrial electron transport chain components (Complexes I–IV) were increased and counteracted the deficit in mitochondrial activity observed in age matched untreated rats [36]. EGCG 30 mg/kg/day can prevent mitochondrial damage in isoproterenol-induced infarcted rats by restoring ATP content and up-regulating the activities of the mitochondrial electron transport chain complexes [37]. Similarly, EGCG rescues cardiac toxicity by restoring the bio-energetic functions of mitochondria in rats exposed to cigarette smoke or sodium fluoride [38, 39]. EGCG targets energy metabolism also by acting as an agonist of AMPK in cellular models [40, 41] and hypercholesterolemic rats [42]. In line with the above evidences, we measured a significant increase in the rate of endogeneous respiration of mitochondria in both GTE and EGCG-treated cardiomyocytes as compared to CTRL cells. The increase in cardiomyocyte oxidative phosphorylation activity, besides explaining the increase in the intracellular ATP content in GTE cardiomyocytes,

suggested that this effect can be ascribed to EGCG.

It should be also noted that sarcoplasmic reticulum (SR) and mitochondria locate close to each other in cardiac muscle cells [26, 43, 44]. This proximity results in a transient exposure of mitochondrial Ca^{2+} uniporter to high concentrations of Ca^{2+} following Ca^{2+} release from the SR favouring the influx of the ion into mitochondria. Mitochondrial calcium accumulation triggers the activation of the metabolic machinery, which increases ATP synthesis in the mitochondria and, hence, ATP levels in the cytosol [27]. It is conceivable that the higher amplitude of the calcium transient measured in GTE cells compared to CTRL might amplify this process, resulting in increased mitochondria ATP production.

We also found a relative rise of the phosphorylated form of PLB in GTE cardiomyocytes compared with CTRL cells, as documented by the higher values of p-PLB/PLB ratio. It is known that the activity of SERCA2 is reversibly regulated by PLB, a 52 amino acid phosphoprotein [27, 45]. Dephosphorylated PLB interacts with SERCA2 and inhibits the pumping activity, whereas phosphorylation of PLB relieves the inhibitory effects resulting in increased calcium re-uptake into the SR and enhanced contractility [46], as we actually observed. On the other hand, our observations are consistent with data published by Kargacin et al [7] who demonstrated that EGCG increases SR Ca^{2+} uptake by altering the transmembrane interaction between SERCA2 and PLB, which in turn depends on the phosphorylation status of the latter. It is well known that the cardiac excitation-contraction coupling is highly dependent on Ca^{2+} transient, that is handled through an array of ion channels, antiporters and pumps that are finally regulated, at post-translational level, by phosphorylation. Many kinases have been implicated in the regulation of Ca^{2+} transient, such as PKA, CamKII and PKC [47-49].

New findings highlight the role, overlooked for many years, of phosphatases in the fine tuning of the phosphorylation balance of physiologically relevant targets [45, 50, 51]. Protein phosphatases-1 (PP1) and -2A (PP2A) are responsible for the dephosphorylation of the majority (more than 90%) of phosphoserine/threonine residues in the cardiac cells [52]. Of note EGCG, possibly through its galloyl group, inhibits the activity of PP1 at physiological achievable concentrations. Comparative docking assay shows that EGCG binds to PP2A in a similar manner, but in a distinct domain [53, 54]. This inhibitory effect of the EGCG on phosphatases might be invoked to explain the higher level of PLB phosphorylation in GTE cardiomyocytes.

We are aware that Ca^{2+} handling not only governs contractile events but can directly or indirectly influence ion channel function in cardiomyocytes, resulting in electrophysiological effects. It is now well recognized that an important component of Na^+ channel regulation is due to Ca^{2+}, calmodulin (CaM) and CaM-dependent protein kinase II (CaMKII) pathway that affects channel function [55]. L-type Ca^{2+} (ICaL) and sodium(Na^+)-Ca^{2+} exchanger currents are Ca^{2+}-sensitive, as well as the slowly activating delayed rectifier current IKs, which plays an important role in regulating action potential duration [56]. Although in this work we did not perform electrophysiological measurements on isolated ventricular myocytes, we can speculate on the potential effects of increased SERCA2 activity, based on several findings reported in the present study. The increased activity of SERCA2 should have increased the SR Ca^{2+} content thereby explaining the enhanced amount of Ca^{2+} released in GTE cardiomyocytes. In the steady state, the increase in the amplitude of the Ca^{2+} transient must exactly balance the acceleration of its decay, in order to maintain intracellular Ca^{2+} homeostasis [27]. We actually observed an increased calcium release associated with an enhanced rate of decay of the Ca^{2+} transient. In addition, we found that diastolic Ca^{2+} levels were unchanged in GTE cardiomyocytes as compared to control cells (Fig. 2). Besides confirming that calcium homeostasis is maintained, even in the presence of a faster SERCA2 calcium re-uptake, this finding should imply no changes in both the intracellular Na^+ concentration that is tightly coupled to calcium concentration regulation (via electrogenic Na^+/Ca^{2+} exchange) and the Ca^{2+}-sensitive IKs current, thus preventing electrophysiological changes promoting arrhythmias. The GTE-induced improvement of cardiomyocyte intrinsic mechanical properties was reflected at the organ level by the high rate of left ventricular pressure decline indicating a faster isovolumic relaxation, coherent with the measurements

at the cellular level. The apparent less evident GTE effects on hemodynamic performance is not surprising by taking into account that cardiac function in the entire animals is influenced by many additional factors in comparison with unloaded isolated myocytes, including the neuro-umoral regulation, the cross talk among cardiac cells and the hemodynamic load.

In conclusion, we have shown that a long term oral administration of physiological doses of GTE increased cardiac contractility and intracellular calcium dynamics of healthy rat cardiomyocytes by enhancing endogenous cardiomyocyte respiration (an EGCG-mediated effect), ATP availability, and PLB phosphorylation resulting in reduced PLB inhibition on SERCA2. Although further studies will be necessary to elucidate the mechanism by which GTE altered PLB phosphorylation and evaluate possible additional action of GTE on other mechanisms modulating SERCA2 activity [27], our findings are of relevance by considering that SERCA2 is recognized as the main player in calcium re-uptake in cardiomyocytes, removing approximately 70-90% of calcium ions from the cytosol in species including humans, mice and rats [57].

Study limitations

We acknowledge some limitations of this study: first, the intracellular molecular mechanisms proposed to explain the enhanced PLB phosphorylation are basically speculative and built on previously reported data; secondly, only steady-state mRNA levels have been provided for L-type Ca^{2+} channel, Na^{+}-Ca^{2+} exchanger, and ryanodine receptor. We cannot rule out the possibility that the GTE might affect the protein expression levels by post-transcriptional mechanisms or modify their biophysical properties by unknown mechanisms, although our data relating to calcium homeostasis do not support this hypothesis.

Acknowledgements

We wish to thank the Tea Solutions, Hara Office Inc. for providing us with green tea extracts.

Disclosure Statement

The authors declare to have no conflict of interests.

References

1 Naponelli V, Ramazzina I, Lenzi C, Bettuzzi S, Rizzi F: Green tea catechins for prostate cancer prevention: present achievements and future challenges. Antioxidants 2017;6:26 DOI:10.3390/antiox6020026.
2 Li YF, Wang H, Fan Y, Shi HJ, Wang QM, Chen BR, Khurwolah MR, Long QQ, Wang SB, Wang ZM, Wang LS: Epigallocatechin-3-Gallate Inhibits Matrix Metalloproteinase-9 and Monocyte Chemotactic Protein-1 Expression Through the 67-κDa Laminin Receptor and the TLR4/MAPK/NF-κB Signalling Pathway in Lipopolysaccharide-Induced Macrophages. Cell Physiol Biochem 2017;43:926-936.
3 Yu NH, Pei H, Huang YP, Li YF: (-)-Epigallocatechin-3-Gallate Inhibits Arsenic-Induced Inflammation and Apoptosis through Suppression of Oxidative Stress in Mice. Cell Physiol Biochem 2017;41:1788-1800.
4 Wang QM, Wang H, Li YF, Xie ZY, Ma Y, Yan JJ, Gao YF, Wang ZM, Wang LS: Inhibition of EMMPRIN and MMP-9 Expression by Epigallocatechin-3-Gallate through 67-kDa Laminin Receptor in PMA-Induced Macrophages. Cell Physiol Biochem 2016;39:2308-2319.
5 Kim HS, Quon MJ, Kim JA: New insights into the mechanisms of polyphenols beyond antioxidant properties; lessons from the green tea polyphenol, epigallocatechin 3-gallate. Redox Biol 2014;2:187-195.
6 Fuchs F, Grabarek Z: The green tea polyphenol (-)-epigallocatechin-3-gallate inhibits magnesium binding to the C-domain of cardiac troponin C. J Muscle Res Cell Motil 2013;34:107-113.
7 Kargacin ME1, Emmett TL, Kargacin GJ: Epigallocatechin-3-gallate has dual, independent effects on the cardiac sarcoplasmic reticulum/endoplasmic reticulum Ca^{2+} ATPase. J Muscle Res Cell Motil 2011;32:89-98.
8 Babu PVA, Sabitha KE, Shyamaladevi CS: Therapeutic effect of green tea extract on oxidative stress in aorta and heart of streptozotocin diabetic rats. Chem Biol Interact 2006;162:114-120.
9 Garcia ML, Pontes RB, Nishi EE, Ibuki FK, Oliveira V, Sawaya AC, Carvalho PO, Nogueira FN, Franco MD, Campos RR, Oyama LM, Bergamaschi CT: The antioxidant effects of green tea reduces blood pressure and sympathoexcitation in an experimental model of hypertension. Hypertens 2017;35:348-354.

10 Friedrich FW, Flenner F, Nasib M, Eschenhagen T, Carrier L: Epigallocatechin-3-Gallate accelerates relaxation and Ca^{2+} transient decay and desensitizes myofilaments in healthy and mybpc3-targeted knock-in cardiomyopathic mice. Front Physiol 2016;7:607. DOI: 10.3389/fphys.2016.00607.
11 Hsieh SR, Tsai DC, Chen JY, Tsai SW, Liou YM: Green tea extract protects rats against myocardial infarction associated with left anterior descending coronary artery ligation. Pflugers Arch 2009;458:631-642.
12 Othman AI, Elkomy MM, El-Missiry MA, Dardor M: Epigallocatechin-3-gallate prevents cardiac apoptosis by modulating the intrinsic apoptotic pathway in isoproterenol-induced myocardial infarction. Eur J Pharmacol 2017;794:27-36.
13 Pan B, Quan J, Liu L, Xu Z, Zhu J, Huang X, Tian J: Epigallocatechin gallate reverses cTnI-low expression-induced age-related heart diastolic dysfunction through histone acetylation modification. J Cell Mol Med 2017;21:2481-2490.
14 Zhang L, Nan C, Chen Y, Tian J, Jean-Charles PY, Getfield C, Wang X, Huang X: Calcium desensitizer catechin reverses diastolic dysfunction in mice with restrictive cardiomyopathy. Arch Biochem Biophys 2015;573:69-76.
15 Lorenz M, Hellige N, Rieder P, Kinkel HT, Trimpert C, Staudt A, Felix SB, Baumann G, Stangl K, Stangl V: Positive inotropic effects of epigallocatechin-3-gallate (EGCG) involve activation of Na^+/H^+ and Na^+/Ca^{2+} exchangers. Eur J Heart Fail 2008;10:439-445.
16 Fujihara T, Nakagawa-Izumi A, Ozawa T, Numata O: High-molecular-weight polyphenols from oolong tea and black tea: purification, some properties, and role in increasing mitochondrial membrane potential. Biosci Biotechnol Biochem 2007;71:711-719.
17 Hotta Y, Huang L, Muto T, Yajima M, Miyazeki K, Ishikawa N, Fukuzawa Y, Wakida Y, Tushima H, Ando H, Nonogaki T: Positive inotropic effect of purified green tea catechin derivative in guinea pig hearts: the measurements of cellular Ca^{2+} and nitric oxide release. Eur J Pharmacol 2006;552:123-130.
18 Robertson IM, Li MX, Sykes BD: Solution structure of human cardiac troponin C in complex with the green tea polyphenol, (-)-epigallocatechin 3-gallate. J Biol Chem 2009;284:23012-23023.
19 Boukhabza M, Hilaly JE, Attiya N, El-Haidani A, Filali-Zegzouti Y, Mazouzi D, Amarouch M-Y: In silico evaluation of the potential antiarrhythmic effect of epigallocatechin-3-gallate on cardiac channelopathies. Comput Math Methods Med DOI: 10.1155/2016/7861653.
20 Savi M, Bocchi L, Mena P, Dall'Asta M, Crozier A, Brighenti F, Stilli D, Del Rio D: *In vivo* administration of urolithin A and B prevents the occurrence of cardiac dysfunction in streptozotocin-induced diabetic rats. Cardiovasc Diabetol 2017;16:80 DOI: 10.1186/s12933-017-0561-3.
21 Bassani JW, Bassani RA, Bers DM: Relaxation in rabbit and rat cardiac cells: species-dependent differences in cellular mechanisms. J Physiol 1994;476:279-293.
22 Barbato S, Sgarbi G, Gorini G, Baracca A, Solaini G: The inhibitor protein (IF1) of the F1F0-ATPase modulates human osteosarcoma cell bioenergetics. J Biol Chem 2015;290:6338-6348.
23 Prasad AM, Inesi G: Silencing calcineurin A subunit reduces SERCA2 expression in cardiac myocytes. Am J Physiol Heart Circ Physiol 2011;300:H173-H180.
24 Hui K, Feng ZP: Efficient experimental design and analysis of real-time PCR assays. Channels (Austin) 2013;7:160-170.
25 Joubert F, Wilding JR, Fortin D, Domergue-Dupont V, Novotova M, Ventura-Clapier R, Veksler V: Local energetic regulation of sarcoplasmic and myosin ATPase is differently impaired in rats with heart failure. J Physiol 2008;586:5181-5192.
26 Kuum M, Kaasik A, Joubert F, Ventura-Clapier R, Veksler V: Energetic state is a strong regulator of sarcoplasmic reticulum Ca^{2+} loss in cardiac muscle: different efficiencies of different energy sources. Cardiovasc Res 2009;83:89-96.
27 Eisner DA, Caldwell JL, Kistamás K, Trafford AW: Calcium and excitation-contraction coupling in the heart. Circ Res 2017;121:181-195.
28 Kang L, Fang Q, Hu SJ: Regulation of phospholamban and sarcoplasmic reticulum Ca^{2+}-ATPase by atorvastatin: implication for cardiac hypertrophy. Arch Pharm Res 2007;30:596-602.
29 Kadambi VJ, Ponniah S, Harrer JM, Hoit BD, Dorn GW, Walsh RA, Kranias EG: Cardiac-specific overexpression of phospholamban alters calcium kinetics and resultant cardiomyocyte mechanics in transgenic mice. J Clin Invest 1996;97:533-539.
30 Chen L, Lee MJ, Li H, Yang CS: Absorption, distribution, and elimination of tea polyphenols in rats. Drug Metab Dispos 1997;25:1045-1050.
31 Kurbitz C, Heise D, Redmer T, Goumas F, Arlt A, Lemke J, Rimbach G, Kalthoff H, Trauzold A: Epicatechin gallate and catechin gallate are superior to epigallocatechin gallate in growth suppression and anti-inflammatory activities in pancreatic tumor cells. Cancer Sci 2011;102:728-734.
32 Osada K, Takahashi M, Hoshina S, Nakamura M, Nakamura S, Sugano M: Tea catechins inhibit cholesterol

oxidation accompanying oxidation of low density lipoprotein *in vitro*. Comp Biochem Physiol C Toxicol Pharmacol. 2001;128:153-164.
33 Kim S, Lee MJ, Hong J, Li C, Smith TJ, Yang GY, Seril DN, Yang CS: Plasma and tissue levels of tea catechins in rats and mice during chronic consumption of green tea polyphenols. Nutr Cancer 2000;37:41-48.
34 Hardie DG, Ross FA, Hawley SA: AMPK: a nutrient and energy sensor that maintains energy homeostasis. Nat Rev Mol Cell Biol 2012;13:251-262.
35 Castellano-González G, Pichaud N, Ballard JW, Bessede A, Marcal H, Guillemin GJ: Epigallocatechin-3-gallate induces oxidative phosphorylation by activating cytochrome c oxidase in human cultured neurons and astrocytes. Oncotarget 2016;7:7426-7440.
36 Srividhya R, Zarkovic K, Stroser M, Waeg G, Zarkovic N, Kalaiselvi P: Mitochondrial alterations in aging rat brain: effective role of (-)-epigallo catechin gallate. Int J Dev Neurosci 2009;27:223-231.
37 Devika PT, Stanely Mainzen Prince P: (-) Epigallocatechingallate protects the mitochondria against the deleterious effects of lipids, calcium and adenosine triphosphate in isoproterenol induced myocardial infarcted male Wistar rats. J Appl Toxicol 2008;28:938-944.
38 Adikesavan G, Vinayagam MM, Abdulrahman LA, Chinnasamy T: (-)-Epigallocatechin-gallate (EGCG) stabilize the mitochondrial enzymes and inhibits the apoptosis in cigarette smoke-induced myocardial dysfunction in rats. Mol Biol Rep 2013;40:6533-6545.
39 Miltonprabu S, Thangapandiyan S: Epigallocatechin gallate potentially attenuates Fluoride induced oxidative stress mediated cardiotoxicity and dyslipidemia in rats. J Trace Elem Med Biol 2015;29:321-335.
40 Collins QF, Liu HY, Pi J, Liu Z, Quon MJ, Cao W: Epigallocatechin-3-gallate (EGCG), a green tea polyphenol, suppresses hepatic gluconeogenesis through 5'-AMP-activated protein kinase. J Biol Chem 2007;282:30143-30149.
41 Zhang HS, Wu TC, Sang WW, Ruan Z: EGCG inhibits Tat-induced LTR transactivation: role of Nrf2, AKT, AMPK signaling pathway. Life Sci 2012;90:747-754.
42 Zhong W, Huan XD, Cao Q, Yang J: Cardioprotective effect of epigallocatechin-3-gallate against myocardial infarction in hypercholesterolemic rats. Exp Ther Med 2015;9:405-410.
43 Bers DM: Calcium cycling and signaling in cardiac myocytes. Annu Rev Physiol 2008;70:23-49.
44 Sharma VK, Ramesh V, Franzini-Armstrong C, Sheu SS: Transport of Ca^{2+} from sarcoplasmic reticulum to mitochondria in rat ventricular myocytes. J Bioenerg Biomembr 2000;32:97-104.
45 Haghighi K, Bidwell P, Kranias EG: Phospholamban interactome in cardiac contractility and survival: A new vision of an old friend. J Mol Cell Cardiol 2014;77:160-167.
46 Frank KF, Bölck B, Erdmann E, Schwinger RH: Sarcoplasmic reticulum Ca^{2+}-ATPase modulates cardiac contraction and relaxation. Cardiovasc Res 2003;57:20-27.
47 Singh RM, Cummings E, Pantos C, Singh J: Protein kinase C and cardiac dysfunction: a review. Heart Fail Rev 2017;22:843-859.
48 Daniels L, Bell JR, Delbridge LM, McDonald FJ, Lamberts RR, Erickson JR: The role of CaMKII in diabetic heart dysfunction. Heart Fail Rev 2015;20:589-600.
49 Johnston AS, Lehnart SE, Burgoyne JR: Ca^{2+} signaling in the myocardium by (redox) regulation of PKA/CaMKII. Front Pharmacol 2015;6:166. DOI: 10.3389/fphar.2015.00166.
50 Heijman J, Dewenter M, El-Armouche A, Dobrev D: Function and regulation of serine/threonine phosphatases in the healthy and diseased heart. J Mol Cell Cardiol 2013;64:90-98.
51 Lubbers ER, Mohler PJ: Roles and regulation of protein phosphatase 2A (PP2A) in the heart. J Mol Cell Cardiol 2016;101:127-133.
52 Lüss H, Klein-Wiele O, Bokník P, Herzig S, Knapp J, Linck B, Müller FU, Scheld HH, Schmid C, Schmitz W, Neumann J: Regional expression of protein phosphatase type 1 and 2A catalytic subunit isoforms in the human heart. J Mol Cell Cardiol 2000;32:2349-2359.
53 Kiss A, Bécsi B, Kolozsvári B, Komáromi I, Kövér KE, Erdődi F: Epigallocatechin-3-gallate and penta-O-galloyl-β-D-glucose inhibit protein phosphatase-1. FEBS J. 2013;280:612-626.
54 Bécsi B, Kiss A, Erdődi F: Interaction of protein phosphatase inhibitors with membrane lipids assessed by surface plasmon resonance based binding technique. Chem Phys Lipids 2014;183:68-76.
55 Chen-Izu Y, Shaw RM, Pitt GS, Yarov-Yarovoy V, Sack JT, Abriel H, Aldrich RW, Belardinelli L, Cannell MB, Catterall WA, Chazin WJ, Chiamvimonvat N, Deschenes I, Grandi E, Hund TJ, Izu LT, Maier LS, Maltsev VA, Marionneau C, Mohler PJ, Rajamani S, Rasmusson RL, Sobie EA, Clancy CE, Bers DM: Na+ channel function, regulation, structure, trafficking and sequestration. J Physiol 2015;593:1347-1360.
56 Kennedy M, Bers DM, Chiamvimonvat N, Sato D: Dynamical effects of calcium-sensitive potassium currents on voltage and calcium alternans. J Physiol 2017;595:2285-2297.
57 Bers DM, Despa S: Cardiac myocytes Ca^{2+} and Na^{+} regulation in normal and failing hearts. J Pharmacol Sci 2006;100:315-322.